Accurate Measurement of Photon Orbital Angular Momentum Carried by Helical Beams Through Spatial Light Modulator

Wang Zheng[1] Xin Jingtao[2] Wu Zhiqiang[1]

[1]*Beijing Institute of Space Mechanics & Electricity, Beijing* 100094, *China*

[2]*School of Optoelectronics, Beijing Institute of Technology, Beijing* 100081, *China*

Abstract A new method is proposed to measure the photon orbital angular momentum (OAM) carried by helical beams accurately through the amplitude computer-generated hologram (CGH) loaded on a liquid crystal display spatial light modulator (LCD-SLM). The diffraction processes of Hermite-Gaussian beams, Laguerre-Gaussian beams and Bessel beams with different orders passing through diffractive optics such as circular aperture, triangular aperture, Young's double-slit, grating whose parameters are adjustable, are simulated with the help of plane wave angular spectrum diffraction formula and Collins formula. Then the propagation properties of helical beams passing through Young's double-slit and triangular aperture are studied by theoretical simulation and experiment, and the measurement of photon OAM carried by helical beams is also realized with those two amplitude diffractive optical elements. Due to the fact that changing and controlling the CGH loaded into the SLM is able to change the configuration, dimension and location of diffractive optical elements flexibly and accurately, the accurate measurement can be achieved conveniently.

Key words holography; laser optics; photon orbital angular momentum; helical beams; computer-generated hologram; spatial light modulator

OCIS codes 090.1970; 140.3295; 050.4865

利用空间光调制器实现螺旋光束轨道角动量的精确测量

王 铮[1] 辛璟焘[2] 邬志强[1]

[1]北京空间机电研究所, 北京 100094

[2]北京理工大学光电学院, 北京 100081

摘要 提出一种利用加载到空间光调制器的振幅型计算全息图精确测量螺旋光束轨道角动量的方法。利用平面波角谱衍射公式和柯林斯公式,对不同阶数的厄米高斯光束、拉盖尔高斯光束、贝塞尔光束经过圆孔、矩孔、三角孔等参数可调的衍射光学元件的衍射过程进行仿真。理论和实验研究了螺旋光束经过杨氏双缝和三角孔后的传输特性,并利用这两种振幅型衍射光学元件实现螺旋光束轨道角动量的测量。由于通过改变和控制加载到空间光调制器上的计算全息图可以方便和高精度地改变光学器件的结构、尺寸、所在的空间位置,因此可便捷地实现螺旋光束轨道角动量的精确测量。

关键词 全息; 激光光学; 光子轨道角动量; 螺旋光束; 计算全息光栅; 空间光调制器

中图分类号 O436.1 **文献标识码** A

doi: 10.3788/LOP52.080902

1 Introduction

Helical beam is a kind of laser beam with helical wavefront structure, which carries the orbital angular momentum (OAM). These characteristics have aroused extensive attention of researchers[1-2]. The Laguerre-Gaussian (LG) beams and high-order Bessel beams are the common helical beams. The helical beams have

收稿日期: 2015-01-05; **收到修改稿日期**: 2015-02-14; **网络出版日期**: 2015-07-11

作者简介: 王 铮(1987—),男,硕士,工程师,主要从事激光光束方面的研究。E-mail: kimiwz@sina.com

a helical phase distribution [exp(i$l\phi$)], each photon carries OAM of $l\hbar$, where l is the quantum number of OAM. The OAM carried by helical beams is able to pass to the particles and then rotate them, which is called 'optical wrench'[3-4]. In addition, since the high-dimensional Hilbert space constructed by photon OAM can increase density and security of the transmission of quantum information[5], the multi-channel information coding and transmission are available by using OAM carried by helical beams[6-10]. Therefore, measurement of the photon OAM carried by helical beams is very important. The common method of measuring the helical beams' OAM uses diffractive optics[11-17] or Mach-Zehnder interferometer[18-19].

In 2006, Sztul *et al.*[12] measured OAM of the helical beams by fixed Young's double-slit successfully. In 2008, Soares *et al.*[13] realized the measurement of beams' OAM through the observation of helical beams diffracted by the triangular aperture. Ghai *et al.*[14] reported the method of single slit diffraction for measuring helical beams' OAM. In 2009, Pu *et al.*[15-16] also measured helical beams' OAM by the Young's double-slit and single-slit. In 2013, Liu[17] found a novel method to detect the OAM by the scattering of helical beam from the weak random scattering screen, but it was just based on simulation.

When using diffractive optics to measure the helical beams' OAM, we need to make the center of diffractive optics and the beam to be measured superposed accurately. In addition, the structure and dimension of the diffractive optics also have influences on the measurement accuracy. However, devices mentioned in Refs. [12-16] were all conventional diffractive optical devices whose structures and dimensions are fixed, and their spatial positions are adjusted by mechanical means. These unfavorable factors have limited accuracy and flexibility of the diffraction method in measuring the photon OAM of the helical beams.

In this paper, the method of generating amplitude diffractive optics from loading the computer-generated hologram (CGH) into a spatial light modulator (SLM) is studied. Due to the fact that changing and controlling the CGH loaded into the SLM are able to change the configurations, dimensions and locations of diffractive optics flexibly and accurately, the accurate measurements can be achieved in this way more conveniently than by mechanical means. Since the dimension and location adjustment accuracy of the diffractive optics are equal to one liquid crystal cell size on SLM, this new method has obvious advantages in accuracy and flexibility of measurement.

2 Generation of amplitude diffractive optics by pure phase modulated LCD-SLM

Nowadays, people usually generate phase diffractive optics by SLM's phase modulation, such as helical phase plates and axicons. In this paper, we generate amplitude diffractive optics by phase modulated LCD-SLM. The main idea is to divide the entire SLM into two areas, corresponding to the transparent and non-transparent areas. The phase modulation of the non-transparent area is a constant value of zero, and the transmittance function $t(x)$ of the transparent area is a parallel phase grating which can be expressed as $t(x)=\exp(\mathrm{i}2\pi x/T)$, where T is the grating constant. The incident beam propagates away from the original direction with a deviation angle of $\theta=\lambda/T$ after the phase grating, but its intensity distribution does not change. Because we use a reflection type SLM, the beam reflected by non- transparent area follows the law of reflection, and the beam reflected by transparent area propagates away from the direction of the law of reflection. Therefore, the beam propagating away from the direction of the law of reflection is equal to the beam propagating through the amplitude diffractive optics. This article achieves the simulation of amplitude diffraction optics by SLM using this method. In the practical application, we have obscured the beam's propagation along the law of reflection, only the beam deviated from the law of reflection is observed[20-21].

With the help of plane wave angular spectrum diffraction formula and Collins formula, we simulate

the diffraction processes of Hermite-Gaussian (HG) beams, LG beams and Bessel beams with different orders passing through adjustable diffractive optics including circular aperture, rectangular aperture, triangular aperture, single slit, Young′s double-slit, grating and etc., as shown in Figs.1 and 2.

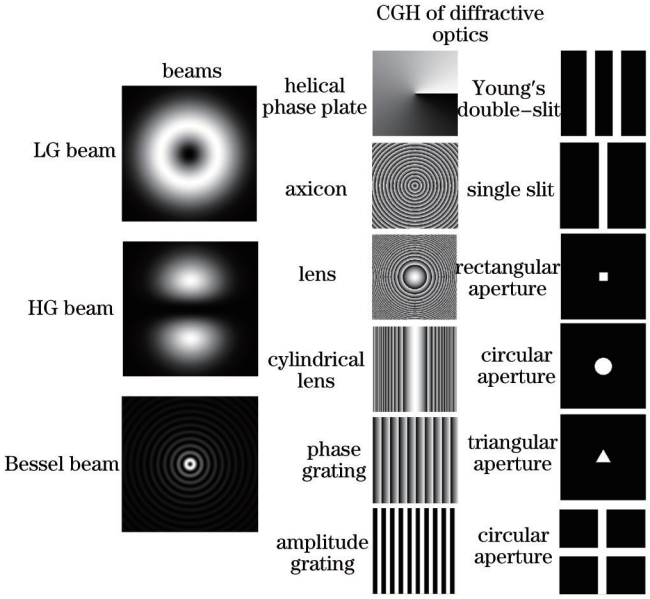

Fig.1 Schematic diagrams of beams and CGHs simulated by the graphical user interface (GUI)

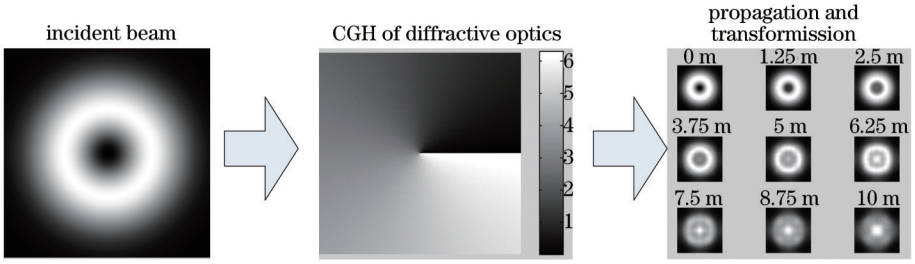

Fig.2 Schematic diagram of the simulation process

3 Simulation results

In this simulation, the LG beam is represented as[1]

$$u(r,\varphi)=C_p^l\exp\left[-\frac{\mathrm{i}kr^2}{2R}-\frac{r^2}{w^2}-\mathrm{i}(2p+l+1)\psi\right]\times\exp(-\mathrm{i}l\varphi)(-1)^p\left(\frac{r}{w}\right)^l L_p^l\left(\frac{2r^2}{w^2}\right),\tag{1}$$

where R represents the radius of curvature of the laser beam wavefront, w represents the radius of the laser beam waist, ψ represents the Gouy phase, p and l represent the radial and azimuthal quantum numbers, respectively, L represents the Laguerre polynomials. In this paper, only the LG beam with the radial quantum number of zero (p=0) is measured.

The distribution of the diffracted beam after amplitude diffractive optics can be obtained by[22]

$$u(x,y)=\mathscr{F}^{-1}\left\{\mathscr{F}\left\{u_0(x_0,y_0)\cdot t(x_0,y_0)\right\}\times H(f_x,f_y)\right\},\tag{2}$$

where x and y are the coordinates on the diffraction screen, $\mathscr{F}$ and $\mathscr{F}^{-1}$ are the two-dimensional Fourier transform functor and the inverse transform functor, respectively, H is the diffraction transfer function in the frequency domain, it can be expressed as

$$H(f_x,f_y)=\exp[\mathrm{i}kd\sqrt{1-(\lambda f_x)^2-(\lambda f_y)^2}],\tag{3}$$

where f_x and f_y are the coordinates of the frequency domain, k=2π/λ.

Based on the above formulas, the simulation can be realized by our GUI. The interface′s parameters are set as follows: Young′s double-slit spacing is 150 pixels (each pixel length of 16 mm), the slit width is

20 pixels ; radius of the circumcircle of the triangular aperture is 90 pixels; the incident beam waist is 3 mm; the incident beam′s wavelength is 0.6328 mm. Figure 3 shows the intensity distributions of the LG_{01} beam propagating after Young′s double-slit and triangular aperture. As the propagation distance increasing, the diffraction field shows certain regularity. For the double-slit interference, the diffraction pattern is relatively clear when the propagation distance is longer than 7 m. For the triangular aperture diffraction, the diffraction pattern is clear when the propagation distance is longer than 5 m. Therefore, if simulations of LG_{01}, LG_{02}, LG_{03}, LG_{0-1} and LG_{0-2} beams are made, the diffraction patterns are needed to be observed at 9 m after double-slit and 7 m after triangular aperture. To shorten the observing distance, a lens was placed before the observation screen. When the lens with focal length of 400 mm was placed at a distance of 600 mm to the diffractive optics, the diffraction patterns would be observed clearly at the focus. The simulation results are shown in Fig.4, the corresponding relations of the diffraction pattern and the photon OAM of the beam can be seen clearly.

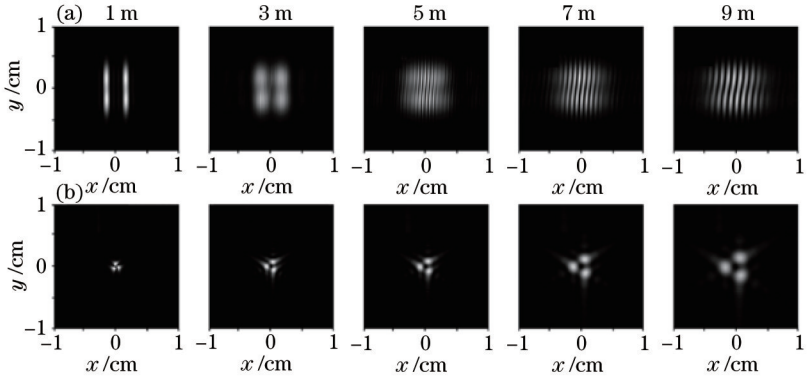

Fig.3 Intensity distributions of the LG_{01} beam propagating after (a) Young′s double-slit, (b) triangular aperture with propagation distances of 1, 3, 5, 7, 9 m

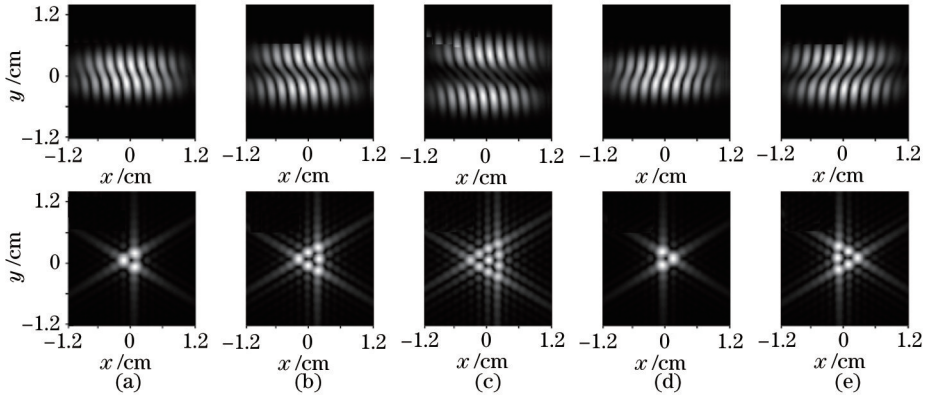

Fig.4 Diffraction patterns of the different modes of LG beam after the double-slit and triangular aperture. (a) LG_{01}; (b) LG_{02}; (c) LG_{03}; (d) LG_{0-1}; (e) LG_{0-2} (The top row corresponds to double-slit; the bottom row corresponds to triangular aperture.)

4 Measurement experiment of photon OAM carried by LG beams

In the experiment, we used the complex binary amplitude grating to generate different modes of LG beam. As shown in Fig.5, when the Gaussian beam irradiated this grating, a 3×3 arrays of LG beam could be generated. In the horizontal direction, LG_{01} and LG_{0-1} beams were generated; In the vertical direction, LG_{03} and LG_{0-3} beams were generated; In the diagonal direction, LG_{02}, LG_{0-2}, LG_{04}, LG_{0-4} beams were generated. And then the generated LG beams were measured by SLM, respectively. The experimental setup is shown in Fig.6, where the fast axis of the polarizer is along the x-direction, because SLM is able to modulate the S-polarized beam only. After the diaphragm′ s selection, the LG beams with different OAMs were measured

chronologically by the CGH on the SLM. The SLM used was the HOLOEYE LC-R2500 LCD-SLM made in Germany and it supplied the software adjusting the location of the CGH during the experiment, so that the incident beam irradiated the center of the grating accurately. Then the +1st-order diffracted beam (the beam was modulated) was filtered out through the SLM by the diaphragm. The final patterns of the light field were recorded by the charge-coupled device (CCD) after the imaging lens.

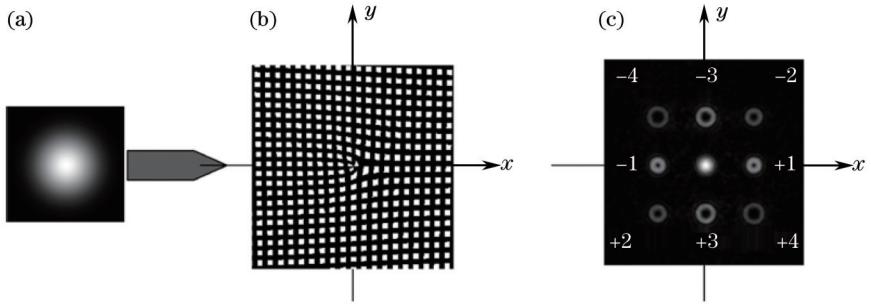

Fig.5 Main diffraction orders′ far-field distribution after the fundamental mode Gaussian beam irradiated the complex binary amplitude grating. (a) Fundamental mode Gaussian beam; (b) complex binary amplitude grating; (c) LG beam arrays

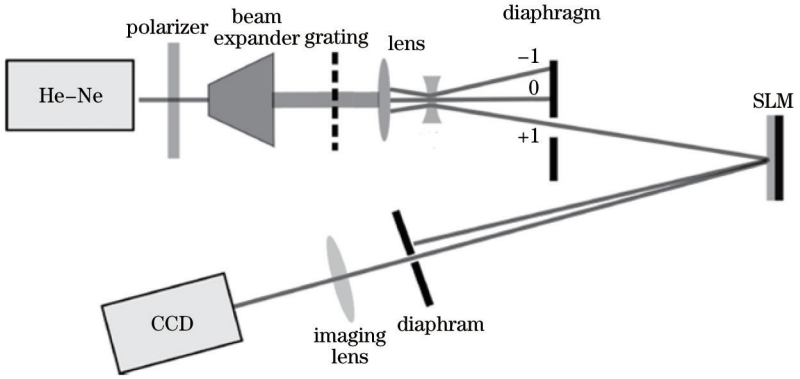

Fig.6 Experimental setup

The experimental results are shown in Fig.7. Compared with the simulated results (Fig.4), the experimental and simulated results are completely complied. As Figs.7(a)~(e) shown, the interference patterns of the LG beam are bended after the double-slit. The degree of bending is related to the photon OAM of the LG beam. The greater the OAM quantum number is, the more obviously bending of the interference pattern occurrs. And the direction of bending is related to positive or negative sign of the OAM quantum number. The bending degree of the entire pattern is close to m times of the fringe spacing, where m is the quantum number of the LG beam′s photon OAM, which is found with the experimental results of Ref.[12].

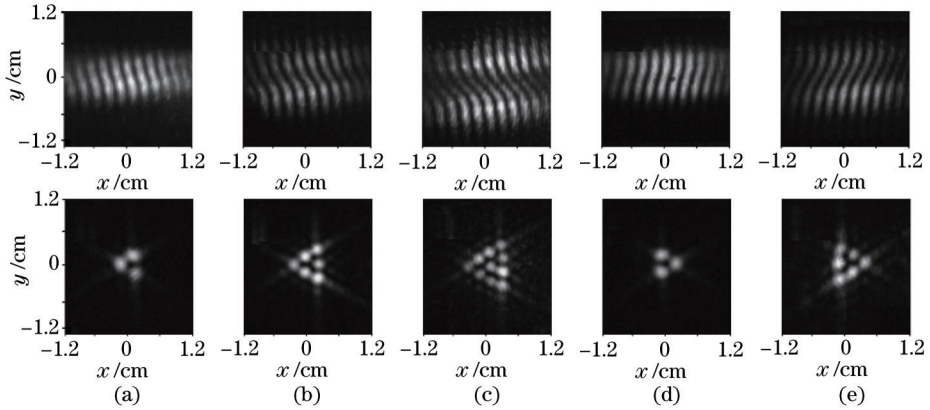

Fig.7 Experimental results of the different modes of LG beam though after the double-slit and triangular aperture. (a) LG_{01}; (b) LG_{02}; (c) LG_{03}; (d) LG_{0-1}; (e) LG_{0-2} (The top row corresponds to double-slit; the bottom row corresponds to triangular aperture.)

As Figs.7(a)~(e) shown, the diffracted fields present equilateral triangle arrays of points after LG beam through the triangular aperture. The points′ number of the triangular array′s one edge is equal to the photon OAM quantum number of LG beam plus 1, and the equilateral triangle′s bottom edge is 30° (the photon OAM is negative) or −30° (the photon OAM is positive) to the horizontal direction, which matches with the result of Ref.[13]. The two methods above-mentioned can be used to measure the photon OAM of helical beam, and also show that the CGH loaded on the phase-type SLM is able to be good simulation of the amplitude-type diffractive optics.

5 Conclusion

A new method is proposed to simulate the amplitude diffractive optics by the CGH loaded on LCD-SLM. In order to facilitate the simulation, a MATLAB interface is derelpoed. Young′s double-slit and triangular aperture are generated on the SLM, and then the measurements of the LG beam′s photon OAM are achieved. Due to the fact that changing and controlling the CGH loaded into the SLM are able to change the configuration, dimension and location of diffractive optical elements flexibly and accurately, the accurate measurement can be achieved conveniently.

References

1 Allen L, Beijersbergen M W, Spreeuw R J C, *et al*.. Orbital angular momentum of light and the transformation of Laguerre-Gaussian laser modes[J]. Phys Rev A, 1992, 45(11): 8185-8189.

2 Lu Xuanhui, Huang Huiqin, Zhao Chengliang, *et al*.. Optical vortex beams and optical vortices[J]. Laser & Optoelectronics Progress, 2008, 45(1): 50-56.
陆璇辉, 黄慧琴, 赵承良, 等. 涡旋光束和光束涡旋[J]. 激光与光电子学进展, 2008, 45(1): 50-56.

3 Simpson N B, Dholakia K, Allen L, *et al*.. Mechanical equivalence of spin and orbital angular momentum of light: an optical spanner[J]. Opt Lett, 1997, 22(1): 52-54.

4 Luo Wei, Cheng Shubo, Yuan Zhanzhong, *et al*.. Power-exponent-phase vortices for manipulating particles[J]. Acta Optica Sinica, 2014, 34(11): 1109001.
罗 伟, 程书博, 袁战忠, 等. 幂指数相位涡旋光束用于微粒操控[J].光学学报, 2014, 34(11): 1109001.

5 Molina T G, Torres J P, Torner L. Management of the angular momentum of light: preparation of photons in multidimensional vector states of angular momentum[J]. Phys Rev Lett, 2002, 88(1): 013601.

6 Bouchal Z, Celechovsḱy R. Mixed vortex states of light as information carriers[J]. New J Phys, 2004, 6: 131.

7 Celechovsḱy R, Bouchal Z. Optical implementation of the vortex information channel[J]. New J Phys, 2007, 9: 328.

8 Celechovsḱy R, Bouchal Z. Generation of variable mixed vortex fields by a single static hologram[J]. Journal of Modern Optics, 2006, 53(4): 473-480.

9 Gao C Q, Qi X Q, Liu Y D, *et al*.. Superposition of helical beams by using a Michelson interferometer[J]. Optics Express, 2010, 18(1): 72-78.

10 Tang Xiaoyan, Gao Kun, Ni Guoqiang. Quantum spectral imaging technology and its prospect in earth observation application[J]. Spaceraft Recovery & Remote Sensing, 2011, 32(5): 80-88.
唐晓燕, 高 昆, 倪国强. 量子光谱成像技术及其在对地观测中的应用前景[J]. 航天返回与遥感, 2011, 32(5): 80-88.

11 Mair A, Vaziri A, Weihs G, *et al*.. Entanglement of the orbital angular momentum states of photons[J]. Nature, 2011, 412: 313-316.

12 Sztul H I, Alfano R R. Double-slit interference with Laguerre-Gaussian beams[J]. Opt Lett, 2006, 31(7): 999-1001.

13 Soares W C, Caetano D P, Fonseca E J S, *et al*.. Direct determination of light beams′ topological charges using diffraction[C]. Lasers and Electro-Optics, 2008, QTuI7.

14 Ghai D P, Vyas S, Senthilkumaran P, *et al*.. Detection of phase singularity using a lateral shear interferometer[J]. Opt Lasers Eng, 2008, 46(6): 419-423.

15 Chen Ziyang, Zhang Guowen, Rao Lianzhou, *et al*.. Determining the orbital angular momentum of vortex Beam by Young′s double-slit interference experiment[J]. Chinese J Lasers, 2008, 35(7): 1063-1067.

陈子阳, 张国文, 饶连周, 等. 杨氏双缝干涉实验测量涡旋光束的轨道角动量[J]. 中国激光, 2008, 35(7): 1063-1067.

16 Wang Tao, Pu Jixiong. Theoretical and experimental study on vortex beam transmitted through a single-slit[J]. Chinese J Lasers, 2009, 36(11): 2902-2907.

王 涛, 蒲继雄. 涡旋光束单缝衍射的理论和实验研究[J]. 中国激光, 2009, 36(11): 2902-2907.

17 Liu Man. Novel method to detect the orbital angular momentum in optical vortex beams[J]. Acta Optica Sinica, 2013, 33(3): 0326002.

刘 曼. 探测涡旋光束轨道角动量的新方法[J].光学学报,2013, 33(3): 0326002.

18 Leach J, Padgett M J, Barnett S M, *et al*.. Measuring the orbital angular momentum of a single photon[J]. Phys Rev Lett, 2002, 88(25): 257901-257904.

19 Gao C Q, Qi X Q, Liu Y D, *et al*.. Sorting and detecting orbital angular momentum states by using a Dove prism embedded Mach-Zehnder interferometer and amplitude gratings[J]. Optics Communications, 2011, 284(1): 48-51.

20 Rong Zhengxin, Guo Chengshan, Zhang Li, *et al*.. Computer-generated holographic phase shifter with liquid crystal display[J]. Chinese J Lasers, 2004, 31(6): 693-697.

荣振宇,国承山,张 莉,等. 液晶光调制计算全息相移器[J]. 中国激光, 2004, 31(6): 693-697.

21 Xin J T, Gao C Q, Li C, *et al*.. Propagation of helical beams through amplitude diffractive optical elements and the measurement of topological charge[J]. Acta Phys Sin, 2012, 61(17): 174202.

辛璟焘, 高春清, 李 辰, 等. 螺旋光束经过振幅型衍射光学元件的传输特性及其拓扑电荷数的测量[J]. 物理学报, 2012, 61(17): 174202.

22 Li Junchang. FFT computation of angular spectrum diffraction formula and its application in wavefront reconstruction of digital holography[J]. Acta Optica Sinica, 2009, 29(5): 1163-1167.

李俊昌. 角谱衍射公式的快速傅里叶变换计算及在数字全息波面重建中的应用[J]. 光学学报, 2009, 29(5): 1163-1167.

栏目编辑: 张 雁